This is the author's accepted manuscript without copyediting, formatting, or final corrections. It will be published in its final form in an upcoming issue of The American Naturalist, published by The University of Chicago Press. Include the DOI when citing or quoting: https://doi.org/10.1086/718643 Copyright 2021 The University of Chicago Press.

Preferential allocation of benefits and resource competition among recipients allows coexistence of symbionts within hosts

Shyamolina Ghosh, Daniel C. Reuman, and James D. Bever[†]

Author Affiliations:

Ghosh: Department of Ecology and Evolutionary Biology and Kansas Biological Survey, The University of Kansas,

1200 Sunnyside Avenue, Lawrence, KS, 66045, USA; email ghoshshyamolina89@gmail.com

Reuman: Department of Ecology and Evolutionary Biology and Kansas Biological Survey, The University of

Kansas, 1200 Sunnyside Avenue, Lawrence, KS, 66045, USA; Laboratory of Populations, Rockefeller University,

1230 York Ave, New York, NY, 10065, USA; email reuman@ku.edu

Bever: Department of Ecology and Evolutionary Biology and Kansas Biological Survey, The University of Kansas,

1200 Sunnyside Avenue, Lawrence, KS, 66045, USA; email jbever@ku.edu (†Corresponding author)

Short Title: Symbiont competition and coexistence

Keywords: preferential allocation, resource competition, species coexistence, negative physiological feedback, stability of mutualism.

Manuscript type: Article

Abstract

Functionally variable symbionts commonly co-occur including within the roots of individual plants, in spite of arguments from simple models of the stability of mutualism that predict competitive exclusion among symbionts. We explore this paradox by evaluating the dynamics generated by symbiont competition for plant resources, and the plant's preferential allocation to the most beneficial symbiont, using a system of differential equations representing the densities of mutualistic and non-mutualistic symbionts and the level of preferentially allocated and non-preferentially allocated resources for which the symbionts compete. We find that host preferential allocation and costs of mutualism generate resource specialization that makes the coexistence of beneficial and non-beneficial symbionts possible. Furthermore, coexistence becomes likely due to negative physiological feedbacks in host preferential allocation. We find that biologically realistic models of plant physiology and symbiont competition predict that the coexistence of beneficial and non-beneficial symbionts should be common in root symbioses, and that the density and relative abundance of mutualists should increase in proportion to the needs of the host.

Introduction

Mutualism is a remarkably common interaction, particularly between plants and their symbionts. However, the persistence of variability in symbiont quality has been identified as a paradox (Heath and Stinchcombe 2014). If hosts reward symbionts indiscriminately and there is a cost to the symbiont for being mutualistic, then non-mutualist fitness will be greater than mutualist fitness and mutualism should decline, as observed in some systems (Bever 2002; Bever et al. 2009; Hart et al. 2013; Porter and Simms 2014). Alternatively, if hosts preferentially allocate resources to the best symbionts (Bever et al. 2009; Jandér and Herre 2010; Ji and Bever 2016; Kiers et al. 2011; Simms et al. 2006; Westhoek et al. 2017) and/or sanction ineffective symbionts (Kiers et al. 2003; Westhoek et al. 2017), then ineffective mutualists should decline. Why then, do mutualists of varying quality commonly coexist?

Partial explanation for the persistence of symbionts of varying quality could arise from heterogeneity in the environment, either generated by variation in hosts ability to discriminate symbionts (Steidinger and Bever 2014) or variation in environmental contexts in which the mutualism benefits their hosts (Moeller and Neubert 2016). In a static environment the joint dynamics of host recognition and host sanctions against ineffective partners can allow the persistence of variation in symbiont quality (Yoder and Tiffin 2017), though host recognition may play only a transient role in mutualism stabilization (Zee and Bever 2014). A general explanation of coexistence of symbionts would necessarily explain the persistence of mutualists of varying quality within the roots of a single host of promiscuous nutritional mutualisms, which include the most common and consequential of plant-symbiont interactions such as mycorrhizae and N-fixation (Bever 2002; Bever et al. 2009; Hart et al. 2013).

The dynamics of mutualism can also be influenced by the patch structure of symbionts, as spatial structure generated by limited dispersal can favor mutualists in pairwise interactions (Mack 2012). When individual hosts interact with many symbionts, spatial structure of the symbionts between hosts does not necessarily favor mutualists (Akçay 2017). However, when spatial structure within hosts increases the fidelity of host investment in beneficial symbionts, then it does favor mutualists (Bever 2015; Bever and Simms 2000). Explicit consideration of symbiont colonization of physiologically independent modules

within hosts, shows that intermediate spatial structure, as represented by mixed colonization of modules (e.g., rhizobia nodules or figs) permits coexistence of beneficial and non-beneficial symbionts in the face of host discrimination (Steidinger and Bever 2016) and this framework has been shown to predict patterns of fig wasp dynamics (Jandér and Steidinger 2017).

Spatial structure enabled fidelity of host investment combined with negative physiological feedback can provide a general explanation of mutualism dynamic and symbiont coexistence in plant-root symbiont interactions (Bever 2015). The rate of host preferential allocation to nutritional mutualists has been shown to scale in proportion to host need (Ji and Bever 2016; Zheng et al. 2015). This can generate negative physiological feedback that reduces plant preferential allocation to beneficial symbionts as beneficial symbionts becomes common, thereby allowing coexistence of beneficial and non-beneficial symbionts. Likelihood of coexistence depends upon for levels of spatial structure within physiologically integrated modules, as represented by the fidelity of plant allocation to the mutualistic symbiont (Bever 2015). This model also implicitly assumed resource competition of symbionts. Such local resource competition can impeded the evolution of traits that produce public benefit (Queller 1992; West et al. 2002), such as increased allocation of host resources. However, local competition may not hinder the evolution of beneficial traits that increase the local carrying capacity (Platt and Bever 2009). Resolving this issue requires explicit consideration of resource competition. Moreover, explicit consideration of symbiont competition could reveal new dynamics. Notably, given that preferential allocation necessarily involves initial non-preferential host investment while forming associations with and evaluating the symbiont, followed by preferential allocation to the most effective mutualist, this sequence creates the possibility of non-beneficial symbionts specializing on the initial investment while beneficial symbionts capitalize on the preferential allocation (Christian and Bever 2018). The potential for symbiont resource competition to influence symbiont coexistence remains unknown.

We develop and analyze a general model of symbiont competition for preferentially allocated and non-preferentially allocated host resources going into the construction and evaluating symbionts. We explicitly test for the first time the potential interactive effects of symbiont resource competition with negative physiological feedback generated from preferential allocation toward mutualists in proportion to host resource need. We show that the stable coexistence of beneficial and non-beneficial symbionts in the model will be commonplace given expected costs. We then use this modeling framework to predict environmental patterns of the efficiency of nutritional mutualisms. We develop the model in the context of arbuscular mycorrhizae, the most common plant nutritional mutualism, though it could also apply to other plant nutritional mutualisms. Construction of models governing the efficiency of mycorrhizal mutualisms is of particular interest as this mutualism can have large impacts on terrestrial ecosystem function and sustainable agriculture through the modulation of plant phosphorus uptake and mediation of carbon sinks in soil.

Model, analytic results, and methods

The densities of two symbionts, a mutualist (M) and a non-mutualist (N), change as a function of their competition for two types of plant resources, the availability of which is represented by the rate of a plant's preferentially allocated carbon to the mutualist (A) and the availability of the plant's construction carbon represented by the plant's uncolonized root-length (R). Construction carbon is thought of as the benefit that fungi receive from the initial colonization of roots. The plant initially invests carbon for the construction of symbiosis structure and the evaluation of symbiont quality, as it cannot recognize the beneficial symbionts until trading commences. Later, the plant preferentially allocates its resources (via A) to the mutualistic symbionts in exchange for phosphorus. We represent the accuracy of preferential carbon allocation by the fidelity (f) of preferential allocation, following Bever (2015). Fidelity depends on the spatial structure of symbiont populations within plant roots, the morphology and modularity of association, and the physiological potential of the plant to allocate resources preferentially to mutualists even in the absence of spatial structures. In our model, fidelity has a theoretical range from 0 to 1, where f = 0 corresponds to high spatial mixing within plant roots or to plants that cannot not allocate preferentially to any specific symbiont, and f = 1 corresponds to high spatial structure within root systems, such that preferentially

allocated carbon is received by the mutualists, M, only. Both symbionts compete with each other to exploit resources. Mutualists have to pay a cost (s) of mutualism, and this cost can reduce the mutualists' maximum growth rate. In mycorrhizal fungi, this cost corresponds to the energetic costs of acquiring, transporting and delivering phosphorus to the host, and is a logical reason for beneficial fungi to be at a competitive disadvantage in mixture with non-beneficial fungi (Bennett and Bever 2009; Bever 2002; Bever et al. 2009; Hart et al. 2013).

The dynamics of the four state variables are then:

$$\frac{dA}{dt} = 1 - P_s - AF(M, N); \tag{1}$$

$$\frac{dR}{dt} = D - (a_M M + a_N N)R; \tag{2}$$

$$\frac{dM}{dt} = \left[\frac{b_{\text{max}}(1-s)C_M}{K+C_M} - d \right] M; \tag{3}$$

$$\frac{dN}{dt} = \left[\frac{b_{\text{max}} C_N}{K + C_N} - d \right] N. \tag{4}$$

Equation (1) represents how carbon allocation rate (A) changes with time depending on phosphorus availability in the soil, scaled to the plant's need (P_s), and the plant's efficiency in taking up phosphorus supplied by the symbionts (F), modified from Bever (2015). As more mutualists colonize the plant's roots, the plant receives more phosphorus per allocated carbon and this increase in efficiency results in the plant needing to allocate less carbon to mycorrhizae (i.e., there is a negative physiological feedback as is consistent with (Ji and Bever 2016; Zheng et al. 2015)). We assume that the efficiency of phosphorus return, F(M, N) in Equation (5), is a saturating function of the density and proportion of mutualists, as shown in Figure 1A.

$$F(M,N) = u \left[\frac{M}{K_A + M} \right] \left[\frac{M/(M+N)}{1 - f + f \left[M/(M+N) \right]} \right], \tag{5}$$

We also show in the Supplement another possible functional form of F(M, N) which gives similar results. By representing soil phosphorus levels within the parameter (P_s) , we can evaluate the dependence of mutualist dynamics on a critical aspect of the environment.

Equation (2) describes how a constant supply rate for construction carbon (represented by root renewal rate, D) is depleted as the roots (R) are colonized by symbionts. Root colonization will correspond to the consumption of construction carbon by the symbionts, and is represented by the linear functional response terms (Equation 2) that are the product of individual symbiont-densities (M, N), their colonization rates (A, A) and the density of uncolonized roots. While both symbiont densities decrease by the same per capita death rate (A) with time, their growth rates (A) are affected differently by costs and preferential allocation as represented in Equation (3) and Equation (4), respectively. Even as fidelity (A) gives an advantage to the mutualist in access to preferentially allocated carbon, the mutualist has to pay an energetic cost (A) which decreases its growth rate on accessed carbon. A0 and A1 in equations (6) and (7) are the total carbon consumed by the mutualist and non-mutualist, respectively, from the plant.

$$C_M = ea_M R + \frac{A}{(M+N)[1-f+f\{M/(M+N)\}]},$$
(6)

$$C_N = ea_N R + \frac{A(1-f)}{(M+N)[1-f+f\{M/(M+N)\}]}$$
 (7)

Each consumed carbon source has two parts: one directly proportional to new root length (R), representing the contribution from construction carbon, and the other part coming from the plant's preferential allocation, a rate that is differentially accessed by symbionts as a function of their proportions as described in Bever (2015). All terms and parameters are described in Table 1. Note that all equations are scaled to plant size (i.e. the changes with plant size are not represented).

In the Supplement, we present a complete derivation of necessary and sufficient conditions for the existence of a positive model equilibrium, $\hat{A} > 0$, $\hat{R} > 0$, $\hat{R} > 0$, $\hat{R} > 0$. Biologically reasonable assumptions on model parameters are also listed there. We here present some concepts that come into play in the derivation and that relate to prior literature. Setting (3) and (4) to zero and solving gives

$$\frac{\hat{A}}{\hat{\alpha}} = -ea_M \hat{R} + \frac{Kd}{b_{\text{max}}(1-s)-d} \tag{8}$$

and

$$\frac{\hat{A}}{\hat{\alpha}} = \frac{-ea_N}{(1-f)}\hat{R} + \frac{Kd}{(b_{\text{max}} - d)(1-f)},\tag{9}$$

where

$$\hat{\alpha} = (\widehat{M} + \widehat{N})[1 - f + f\{\widehat{M}/(\widehat{M} + \widehat{N})\}]. \tag{10}$$

This suggests consideration of the two equations

$$y = -ea_{M}x + \frac{Kd}{b_{\max}(1-s) - d}$$
 (11)

and

$$y = \frac{-ea_N}{(1-f)}x + \frac{Kd}{(b_{\text{max}} - d)(1-f)}$$
 (12)

where,
$$x = \hat{R}$$
, $y = \frac{\hat{A}}{\hat{g}}$ (13)

which are plotted schematically in Fig. 1B. These are similar to zero net growth isoclines (ZNGI), though they differ from standard ZNGIs because the axes do not correspond to state variables in our system of dynamical equations. Nevertheless, reasonable biological assumptions ($a_N \ge a_M$, s > 0, $b_{\text{max}} - d > 0$, $b_{\text{max}}(1-s) - d > 0$, 0 < f < 1) imply (Supplement) that the x intercept of (11) is strictly to the right of the x intercept of (12), and the slope of (12) is strictly steeper (more negative) than the slope of (11). Thus the lines (11) and (12) have a positive intersection point if and only if the y intercept of (12) is strictly greater than the y intercept of (11). This leads to the following necessary condition for the existence of a positive model equilibrium:

$$f_{\min} < f \tag{14}$$

where we define

$$f_{\min} = \frac{sb_{\max}}{(b_{\max} - d)}.$$
 (15)

Christian and Bever (2018) inferred a similar condition with a graphical representation of competition. We furthermore find (Supplement) that there exists a quantity f_{max} such that the conditions

$$f_{\min} < f < f_{\max} \tag{16}$$

are both necessary and sufficient for the model to have a positive dynamical equilibrium. For $f < f_{\min}$, non-mutualists outcompete mutualists, whereas for $f > f_{\max}$ mutualists outcompete non-mutualists. Although this condition does not guarantee that the model equilibrium is a stable equilibrium, extensive Monty Carlo simulations (Supplement) illustrated that stability of this equilibrium is extremely common and may be universal under the assumptions listed in the Supplement.

To illustrate our analytical results, we carried out simulations of model dynamics using various values of P_s and various values of f in three different ranges, i.e., $f < f_{\min}$, f within the interval (f_{\min}, f_{\max}) , and $f > f_{\max}$. In all cases we solved equations (1) to (4) numerically by the classic 4th order Runge-Kutta method with time increment $\Delta t = 0.01$ and initial values for A, R, M, and N equal to 0.5, 0.5, 0.1 and 0.1, respectively. For all parameter combinations, the model was simulated for long enough to reach steady state. For all simulations and other calculations, certain parameter values were always kept at fixed values, namely, u = 0.4, $b_{\max} = 0.8$, d = 0.5, e = 0.5, e = 0.5, e = 0.5, and e = 0.5. From now on we will call these the "default parameter values" for these parameters.

Numeric results

Model simulations illustrated our analytical result (see *Model, analytic results, and methods*, and the Supplement for the mathematical details) are consistent with the condition $f_{\min} < f < f_{\max}$ being necessary and sufficient for the existence of a positive model dynamical equilibrium; our simulations illustrated that when $f < f_{\min}$, the non-mutualist (N) outcompetes the mutualist (M), and when $f > f_{\max}$, the mutualist outcompetes the non-mutualist. For example, when f was below f_{\min} in our simulations (Fig. 2A-B), co-existence was not possible as the lines (11) and (12) did not intersect in the positive quadrant of the Euclidean plane (Fig. 2A). The model trajectory in $(A/\alpha, R)$ phase space (Fig. 2A, dashed line) showed that uncolonized roots (R) became depleted over time (see also Fig. 2B). The plant continued to increase its rate of allocation to the symbionts, in search of mutualists, but because the fidelity of allocation to the

mutualists was low, increased allocation only helped the non-mutualists to rapidly become much more abundant than the mutualists (Fig. 2B). Figs 2C-D illustrated that coexistence was possible when $f_{\min} < f < f_{\max}$. The lines (11) and (12) intersected in the upper right quadrant (Fig. 2C). Figs. 2E-F illustrated a case with $f > f_{\max}$. A positive solution to equations (11) and (12) was found (Fig. 2E), but it corresponded to a non-positive N, indicating that the mutualist outcompeted the non-mutualist (Fig. 2F).

We explored an example of how the equilibrium values $(\hat{A}, \hat{R}, \hat{M}, \hat{N})$ changed with variation of soil phosphorous, P_s , and fidelity of preferential allocation, f (Fig. 3). For the parameters we used, with increasing soil phosphorus availability (P_s) , the plant reduced its preferential allocation at equilibrium, \hat{A} , consistent with more of plant need being met from direct intake from soil and therefore less need for trading with the mutualist (Fig. 3A). This, in turn, led to reduced prevalence of the mutualist relative to the non-mutualist (Fig. 3B). Larger values of f within the range (f_{\min}, f_{\max}) led to increased prevalence of the mutualist relative to the non-mutualist at equilibrium, as expected, as well as a reduced rates of plant preferential allocation consistent with greater efficiency of trade with higher proportion of mutualist (Fig. 3C, D). The model equilibrium and coexistence were always locally asymptotically stable as ensured by the negative real part of the eigenvalues of the Jacobian evaluated at the equilibrium. For the results of Fig. 3, only one of the two parameters P_s and f was varied at a time, while the other was kept fixed. To understand the relative abundance of the mutualist and non-mutualist for all combinations of P_s and f for which coexistence was possible, we plotted $P_M = \hat{M}/(\hat{M} + \hat{N})$ against P_s and f (Fig. 4), keeping other parameters fixed as in Fig. 2. P_M varied between 0 and 1.

Finally, we examined the influence of the rate of production of new roots, D, on coexistence. For the parameters we examined, higher production of new roots led to a wider range of fidelity of plant allocation (f) for which coexistence was possible, and that was the case regardless of whether the cost of mutualism was manifested through a reduced growth rate for mutualists (i.e., s > 0) or whether it was manifested through reduced rates of colonization of new roots (i.e., $a_M < a_N$), or both (Fig. 5). Moreover, the interacting effects of D, relative new-root colonization rates (a_M, a_N), and the growth cost of mutualism

(s) on f_{max} suggest that differential colonization ability ($a_M < a_N$) could be very important for promoting coexistence, especially for larger D and smaller s (compare Fig. 5A, C). When both symbionts had equal colonization rates of new roots ($a_M = a_N$), then the range of f for which coexistence was possible (f_{\min} , f_{\max}), was only substantially large when the growth cost of mutualism, s, was high, as the growth cost of mutualism was the only mechanism by which the non-mutualist had a competitive advantage (Fig. 5C, D).

Discussion

The forces governing stability of mutualisms and maintenance of diversity in symbiont quality is a central problem in evolutionary ecology (Heath and Stinchcombe 2014). We identify that preferential allocation to the most efficient mutualist can counter costs of mutualism, allowing persistence of mutualists and resulting in coexistence of mutualists and non-mutualists across a broad range of conditions. Coexistence results from the interaction of the complementary forces of resource partitioning and a negative physiological feedback. Resource partitioning results from mutualists having greater access to preferentially allocated carbon (provided f > 0), while non-mutualists have the higher competitive ability on non-preferentially allocated carbon, i.e., new root growth (provided s > 0). Previous work identified a necessary condition for coexistence via resource partitioning (Christian and Bever 2018) under the standard assumptions of resource ratio theory. However, from zero net growth isoclines alone (Fig. 1b), one would predict such resource partitioning to be rare, as only a narrow band of resource supply points would allow coexistence. We show that when plants allocate to the mutualist in proportion to their need, supply rates of preferentially allocated carbon change over time and move the supply point to the region of coexistence. Negative physiological feedback acts as a stabilizing force that expands the likelihood of coexistence of symbionts of varying degrees of mutualism. By deriving the general conditions for coexistence of symbionts under resource competition in systems of preferential allocation, we identify that coexistence is likely under biologically realistic parameters.

Our model differs from classic resource competition models, and our results differ from inferences from the classic models regarding the limiting similarity sufficient to allow coexistence of competitors. In earlier studies (Macarthur and Levins 1967; MacArthur 1984; Tilman 1982), researchers classically argued that species with a similar niche, as defined by their zero growth isoclines, can only coexist when tradeoffs cause crossing of these isoclines and when the resources are supplied within the narrow confines of their consumption vectors as shown in Fig. 1B. In our system, the cost of mutualism and the fidelity of investment determine the trade-offs and crossing of the zero growth isoclines (Fig. 2C). The consumption vectors mapped onto this cross point, may circumscribe a narrow band of supply points, yet coexistence occurs under broader conditions because negative physiological feedback moves the supply point of allocated carbon to within this range at equilibrium. Therefore, the coexistence of mutualistic and non-mutualistic symbionts may be more likely than might be expected from competing species in other systems.

Mutualisms have been likened to systems of cooperation (Bronstein 2001). Our system can be described as a literal system of cooperation among symbionts when fidelity of investment (f) is less than 1 because the mutualist is creating a public benefit as (1-f) of the preferentially allocated carbon is equally available to all symbionts. Biologically, f < 1 corresponds to some level of mixing of symbionts (e.g. via dispersal) within the host root system. Given limited symbiont dispersal, the benefit of host investment in mutualists is likely to go to kin (Bever and Simms 2000). Simple evolutionary models have suggested that the evolution of cooperation in systems of local dispersal (as would be true for symbionts) can be limited by competition with non-cooperators (Queller 1992; West et al. 2002). However, when the cooperative act increases local carrying capacity (i.e. there is population elasticity), as we show is the case for increased plant preferential allocation, then the cooperative/mutualist trait can be favored even given local competition among kin (Platt and Bever 2009). We demonstrate that a more complete model of resource competition that includes both public goods from host preferential allocation and resource driven negative density dependence, yields population elasticity and a high likelihood of persistence of the cooperative trait and coexistence with the non-cooperative trait. Our model result showing a central role of spatial structure

of symbionts within plant roots systems (i.e. f must be greater than f_{\min}) for the persistence of the beneficial root symbionts is consistent with empirical observations (Bever et al. 2009).

Relevance of model results to plant-mycorrhizal dynamics:

Given their role in modulating plant nutrition, mycorrhizal fungal dynamics are critical to terrestrial carbon dynamics and validated models are necessary to predict these terrestrial responses to anthropogenic perturbations. Our model represents an advance in this direction, as we build on basic aspects of the plantmycorrhizal fungal biology that are capable of governing the efficiency of the mycorrhizal mutualism in the face of competition from non-beneficial symbionts (cheaters). Our model includes the energetic costs of trading with the fungus as a dynamic variable, in contrast to other formulations (Lu and Hedin 2019). Integrating the dynamics of these costs and the benefits of trading described here into models of plant growth would advance understanding of plant microbiome function potential impacts on terrestrial productivity. Moreover, potential feedbacks between plant growth and AM fungal dynamics could modify predictions made by our model. Nevertheless, our model generates qualitative predictions on the efficiency of the mycorrhizal mutualism that are consistent with empirical patterns. As predicted by the model, the mycorrhizal communities become less mutualistic with increasing soil resources (Boerner 1990; Corkidi et al. 2002; Johnson 1993; Louis and Lim 1988) and more mutualistic with increasing levels of aboveground resource (Klironomos et al. 2005) which is expected to increase plant demand for soil resources, and hence plant preferential allocation rates. Interestingly, our model identifies a high likelihood that non-mutualists can coexist with mutualists even under low levels of soil P.

Plant root architecture has been shown to correlate with the dependence of plants on mycorrhizal fungi, as finer rooted phenotypes benefit less from mycorrhizal fungi than coarsely rooted phenotypes (Seifert et al. 2009; Koziol and Bever 2015). Bever (2015) had posited that finely rooted phenotypes may have reduced control on non-beneficial symbionts because of reduced spatial independence in the fine root system would lead to reduced fidelity of preferential allocation. Here, we identify an independent reason that finely rooted plant phenotypes may enable non-mutualists. Fine root systems have greater root length,

which would correspond to increased opportunity for non-mutualists to outcompete mutualists for initial root colonization and the benefits of plant investments in construction costs. Our model confirms that increased construction costs inputs disproportionately advantages non-mutualists (Fig. 5C). Empirical tests of these novel theoretical predictions are necessary.

Finally, our model identifies that non-mutualists will be selected to increase dispersal and infection rates. While general models of mutualists have produced similar predictions for cheaters (Mack 2012), our model illustrates the importance of the dispersal and root infection for the success of non-beneficial AM fungi, as they may be viewed as infection specialists, as supported by (Bennett and Bever 2009). While all AM fungi disperse locally through hyphal extension, some fungal taxa produce sporocarps that can be dispersed through small mammals (Mangan and Adler 2002) or an abundance of small spores that may be more likely to disperse with wind erosion (Chaudhary et al. 2020). Our results predict that dispersal traits may be particularly important for non-beneficial AM fungi. It is currently unknown whether fungi with greater dispersal abilities are generally less beneficial than other AM fungi.

Relevance of model results to dynamics of other mutualists:

Our results are directly relevant to the dynamics of host-symbiont systems with preferential allocation toward symbionts in proportion to host need. This includes legume-rhizobia interactions, where preferential allocation has been demonstrated (Simms et al. 2006; Westhoek et al. 2017) and preferential allocation has been shown to be reduced by N fertilization (Oono et al. 2020). Dynamics of other plant nutritional mutualisms are also likely to be represented by our model, as plant root systems physiologically integrate anatomically modular symbiotic associations (e.g. associations in different root branches). The extent to which other mutualisms share these features remains to be demonstrated. Fig wasp pollination mutualisms share preferential allocation to modular interactions (Jandér and Herre 2010; Jandér and Steidinger 2017), however it is not obvious that strength of preferential allocation to fertilized fruits will be modulated in way that would generate negative physiological feedback. Coral-algal and lichen symbioses also have modularity, however it remains to be demonstrated that coral or lichen fungi are sufficiently physiological

integrated to support preferential allocation. More generally, our work joins recent work showing that

understanding the competitive context of mutualists is critical to understanding the stability and trajectory

of mutualisms (Johnson and Bronstein 2019; Koffel et al. 2021).

Summary

Counter to inference from simple models of preferential allocation and evolution of cooperation, we find

that beneficial and non-beneficial (i.e. cheater) symbionts are likely to coexist within plant nutritional

mutualisms. Our explicit model shows that coexistence of functionally different symbionts is likely because

host regulation of the supply rate of preferentially allocated carbon increases the likelihood of resource

partitioning of preferentially-allocated and construction carbon. Our model forms a foundation for the

heuristic understanding of symbiont dynamics, the influence of root architecture on the stability of

mutualism, and qualitative predictions of the response of ecologically critical plant-symbiont mutualisms

to environmental perturbations.

Acknowledgements

We thank Erol Akçay, Jennifer Lau, John Vandermeer, and two anonymous reviewers for their helpful

suggestions. SG and DCR are supported by a grant from the James S McDonnell Foundation, grant 1714195

from the National Science Foundation (NSF), and a grant from the California Department of Fish and

Wildlife Delta Science Program. JDB acknowledges support from NSF grants DEB 1556664, DEB

1738041 and OIA 1656006.

Statement of Authorship

SG and JDB conceptualized the research; SG, DCR, and JDB set up the model formulation, SG

performed analytical and numerical analyses; DCR performed simulation for local asymptotic

15

stability analysis. SG and JDB wrote the first draft of the manuscript; all authors contributed to and approved the final version of the manuscript.

Data and Code Availability

All R and Fortran code and datasets required to replicate the analyses are available in the Dryad Digital Repository (https://doi.org/10.5061/dryad.zw3r2288m) and also in GitHub repository (https://github.com/sghosh89/CMN).

Literature Cited

- Akçay, E. 2017. Population structure reduces benefits from partner choice in mutualistic symbiosis. Proceedings of the Royal Society B 284:20162317.
- Bennett, A. E., and J. D. Bever. 2009. Trade-offs between arbuscular mycorrhizal fungal competitive ability and host growth promotion in *Plantago lanceolata*. Oecologia 160:807-816.
- Bever, J. D. 2002. Negative feedback within a mutualism: host–specific growth of mycorrhizal fungi reduces plant benefit. Proceedings of the Royal Society B 269:2595-2601.
- Bever, J. D. 2015. Preferential allocation, physio-evolutionary feedbacks, and the stability and environmental patterns of mutualism between plants and their root symbionts. New Phytologist 205:1503-1514.
- Bever, J. D., S. C. Richardson, B. M. Lawrence, J. Holmes, and M. Watson. 2009. Preferential allocation to beneficial symbiont with spatial structure maintains mycorrhizal mutualism. Ecology Letters 12:13-21.
- Bever, J. D., and E. L. Simms. 2000. Evolution of nitrogen fixation in spatially structured populations of *Rhizobium*. Heredity 85:366-372.
- Boerner, R. E. 1990. Role of mycorrhizal fungus origin in growth and nutrient uptake by *Geranium robertianum*. American Journal of Botany 77:483-489.

- Bronstein, J. L. 2001. The exploitation of mutualisms. Ecology Letters 4:277-287.
- Chaudhary, B., S. Nolimal, M. A. S. Hernandez, C. Egan, and J. Kastens. 2020. Trait-based aerial dispersal of arbuscular mycorrhizal fungi. bioRxiv.
- Christian, N., and J. D. Bever. 2018. Carbon allocation and competition maintain variation in plant root mutualisms. Ecology and Evolution 8:5792-5800.
- Corkidi, L., D. L. Rowland, N. C. Johnson, and E. B. Allen. 2002. Nitrogen fertilization alters the functioning of arbuscular mycorrhizas at two semiarid grasslands. Plant and Soil 240:299-310.
- Hart, M. M., J. Forsythe, B. Oshowski, H. Bücking, J. Jansa, and E. T. Kiers. 2013. Hiding in a crowd—does diversity facilitate persistence of a low-quality fungal partner in the mycorrhizal symbiosis? Symbiosis 59:47-56.
- Heath, K. D., and J. R. Stinchcombe. 2014. Explaining mutualism variation: a new evolutionary paradox? Evolution 68:309-317.
- Jandér, K. C., and E. A. Herre. 2010. Host sanctions and pollinator cheating in the fig tree–fig wasp mutualism. Proceedings of the Royal Society B 277:1481-1488.
- Jandér, K. C., and B. S. Steidinger. 2017. Why mutualist partners vary in quality: mutation—selection balance and incentives to cheat in the fig tree—fig wasp mutualism. Ecology letters 20:922-932.
- Ji, B., and J. D. Bever. 2016. Plant preferential allocation and fungal reward decline with soil phosphorus: implications for mycorrhizal mutualism. Ecosphere 7:e01256.
- Johnson, C. A., and J. L. Bronstein. 2019. Coexistence and competitive exclusion in mutualism. Ecology 100:e02708.
- Johnson, N. C. 1993. Can fertilization of soil select less mutualistic mycorrhizae? Ecological applications 3:749-757.
- Kiers, E. T., M. Duhamel, Y. Beesetty, J. A. Mensah, O. Franken, E. Verbruggen, C. R. Fellbaum et al. 2011. Reciprocal rewards stabilize cooperation in the mycorrhizal symbiosis. Science 333:880-882.

- Kiers, E. T., R. A. Rosseau, S. A. West, and R. F. Denison. 2003. Host sanctions and the legume-rhizobium mutualism. Nature 425:78-81.
- Klironomos, J. N., M. F. Allen, M. C. Rillig, J. Piotrowski, S. Makvandi-Nejad, B. E. Wolfe, and J. R. Powell. 2005. Abrupt rise in atmospheric CO 2 overestimates community response in a model plant–soil system. Nature 433:621.
- Koffel, T., T. Daufresne, and C. A. Klausmeier. 2021. From competition to facilitation and mutualism: a general theory of the niche. Ecological Monographs 91:e01458.
- Louis, I., and G. Lim. 1988. Differential response in growth and mycorrhizal colonisation of soybean to inoculation with two isolates of Glomus clarum in soils of different P availability. Plant and Soil 112:37-43.
- Lu, M., and L. O. Hedin. 2019. Global plant–symbiont organization and emergence of biogeochemical cycles resolved by evolution-based trait modelling. Nature ecology & evolution 3:239.
- Macarthur, R., and R. Levins. 1967. The Limiting Similarity, Convergence, and Divergence of Coexisting Species. American Naturalist 101:377-385.
- MacArthur, R. H. 1984. Geographical ecology: patterns in the distribution of species. Princeton University Press.
- Mack, K. M. 2012. Selective feedback between dispersal distance and the stability of mutualism. Oikos 121:442-448.
- Mangan, S. A., and G. H. Adler. 2002. Seasonal dispersal of arbuscular mycorrhizal fungi by spiny rats in a neotropical forest. Oecologia 131:587-597.
- Moeller, H. V., and M. G. Neubert. 2016. Multiple friends with benefits: an optimal mutualist management strategy? American Naturalist 187:E1-E12.
- Oono, R., K. E. Muller, R. Ho, A. Jimenez Salinas, and R. F. Denison. 2020. How do less-expensive nitrogen alternatives affect legume sanctions on rhizobia? Ecology and Evolution 10:10645-10656.
- Platt, T. G., and J. D. Bever. 2009. Kin competition and the evolution of cooperation. Trends in ecology & evolution 24:370-377.

- Porter, S. S., and E. L. Simms. 2014. Selection for cheating across disparate environments in the legume-rhizobium mutualism. Ecology Letters 17:1121-1129.
- Queller, D. C. 1992. A general model for kin selection. Evolution 46:376-380.
- Simms, E. L., D. L. Taylor, J. Povich, R. P. Shefferson, J. L. Sachs, M. Urbina, and Y. Tausczik. 2006. An empirical test of partner choice mechanisms in a wild legume-rhizobium interaction. Proceedings of the Royal Society B 273:77-81.
- Steidinger, B. S., and J. D. Bever. 2014. The Coexistence of Hosts with Different Abilities to Discriminate against Cheater Partners: An Evolutionary Game-Theory Approach. American Naturalist 183:762-770.
- Steidinger, B. S., and J. D. Bever. 2016. Host discrimination in modular mutualisms: a theoretical framework for meta-populations of mutualists and exploiters. Proceedings of the Royal Society B 283:20152428.
- Tilman, D. 1982. Resource Competition and Community Structure. Princeton, NJ, Princeton University Press.
- West, S. A., I. Pen, and A. S. Griffin. 2002. Cooperation and competition between relatives. Science 296:72-75.
- Westhoek, A., E. Field, F. Rehling, G. Mulley, I. Webb, P. S. Poole, and L. A. Turnbull. 2017. Policing the legume-Rhizobium symbiosis: a critical test of partner choice. Scientific Reports 7:1419.
- Yoder, J. B., and P. Tiffin. 2017. Sanctions, partner recognition, and variation in mutualism. American Naturalist 190:491-505.
- Zheng, C., B. Ji, J. Zhang, F. Zhang, and J. D. Bever. 2015. Shading decreases plant carbon preferential allocation towards the most beneficial mycorrhizal mutualist. New Phytologist 205:361-368.

TableTable 1: Description of model terms.

Term	Definition	Values	Units	
Variables				
A	Rate of preferential carbon allocation to the mutualists	>0	Carbon unit/time	
R	Length of new roots available for colonization by symbionts	>0	Length	
M	Density of mutualist symbiont	>0	Hyphae/volume	
N	Density of non-mutualist symbiont	>0	Hyphae/volume	
Functions				
F(M,N)	Function representing phosphorus uptake by both symbionts	Phosphorous/Carbon unit		
C_{M}	Carbon consumed by mutualist (per capita)	>0	Carbon unit/(symbiont*time)	
C_N	Carbon consumed by non-mutualist (per capita)	>0	Carbon unit/(symbiont*time)	
Parameters				
D	Constant new root growth rate	>0	Length/time	
a_{M}	Colonization rate of new roots by mutualists	(0,1)	1/(symbiont * time)	
a_N	Colonization rate of new roots by non-mutualists	(0,1)	1/(symbiont * time)	
e	Construction carbon available by the plant per colonized root	(0,1)	C-unit / root-length	
P_{s}	Phosphorus intake rate from soil scaled to the plant's need	(0,1)	Phosphorous /time	
и	Phosphorus-exchange for the mutualists per Carbon unit from the plant	(0,1)	Phosphorous /Carbon unit	
f	Fidelity of the plant's allocation to the mutualist symbionts	(0,1)	-	
S	Cost of mutualism	(0,1)	-	
b_{max}	Maximum growth rate of symbionts per capita	>0	1/time	
d	Death rate of symbionts per capita	(0,1)	1/time	
K_A	Half-saturation constant for mutualist	>0	Symbiont density	
K	Half-saturation constant for allocated carbon	>0	C-unit	

Figure Legends

Figure 1: (A) P-uptake via mycorrhizal fungi, F(M, N), as a saturating function of densities of mutualists

(M) and non-mutualists (N). Parameters used: f = 0.3, u = 0.4, $K_A = 5$. (B) Schematic diagram depicting

reasoning that leads to a necessary condition for the existence of a positive model equilibrium (Model,

analytic results, and methods). The lines are given by equations (11) for mutualist and (12) for non-

mutualist, where x and y axes labels are \hat{R} and $\hat{A}/(\hat{\alpha})$, respectively (see Eq. 13). Under biologically

reasonable constraints on parameter values (Supplement), the x intercept of (11) is strictly to the right of

the x intercept of (12), and the slope of (12) is strictly steeper (more negative) than the slope of (11).

Therefore, the lines intersect in a positive point if an only if the y intercept of (12) is strictly greater than

the y intercept of (11), which leads to the necessary condition (14) in Model, analytic results, and methods.

Arrows represent the consumption vectors reflecting the two resources being consumed in proportion to

their access.

Figure 2: Simulations of model dynamics for example f values. Parameter values $P_s = 0.3$, s = 0.1, $a_M = 0.1$

0.1, $a_N = 0.2$, D = 5, and the default parameters of *Model, analytic results, and methods* were used in all

simulations. For these parameters, $f_{\min} = 0.267$ and $f_{\max} = 0.495$. For $f < f_{\min}$ (A-B; f = 0.2 was

used), the non-mutualist won in competition. For f chosen so that $f_{\min} < f < f_{\max}$ (C-D; f = 0.3 was

used) both symbionts could coexist. For f chosen so that $f > f_{\text{max}}$ (E-F; f = 0.6 was used), the mutualist

dominated. Dotted trajectories with arrowhead in (A), (C), and (E) show the time evolution of A/α and R,

where $\alpha = (M + N)[1 - f + f(M/((M + N)))]$. Panel (B), (D), (F) have two y axes: left side axis (in

black) shows variation of A and R, and right-side axis (in magenta) shows variation of symbionts with time;

21

axes are color-coded as with the figure legends.

Figure 3: Results showing how the model equilibrium $(\hat{A}, \hat{R}, \hat{M}, \hat{N})$ changed with variation of soil-

phosphorous, P_s , and fidelity, f. For (A-B), f was fixed at 0.3, and P_s was varied from 0 to 1. For (C-D),

 P_s was fixed at 0.3, and f was varied from $f_{min} (= 0.267)$ to $f_{max} (= 0.495)$. Negative values of

Max(Re(eigenvalues)) ensured that the model equilibrium was locally asymptotically stable. Other

parameters were same as in Fig. 2.

Figure 4: Regime of co-existence of the symbionts for the full range of f and P_s , where parameters other

than f and P_s took values as given in *Model, analytic results, and methods* and in the caption of Fig. 2.

Color shows the proportional abundance of the mutualist, P_M , at model equilibrium, i.e., $\widehat{M}/(\widehat{M}+\widehat{N})$. For

the parameters used, f_{\min} was constant, equal to 0.267.

Figure 5: Regime of co-existence of the symbionts: variation in the range for coexistence (f_{\min}, f_{\max})

against the new root growth rate, D. Color shows the proportional abundance of the mutualist, P_M , at model

equilibrium, i.e., $\widehat{M}/(\widehat{M}+\widehat{N})$ similar to Fig. 4. (A, B) with $a_M < a_N$ (C, D) with $a_M = a_N$ (B). Parameters

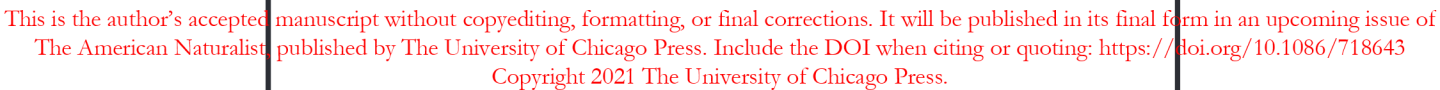
were $P_s = 0.3$ and the default parameter set of *Model, analytic results, and methods*. All plots show that

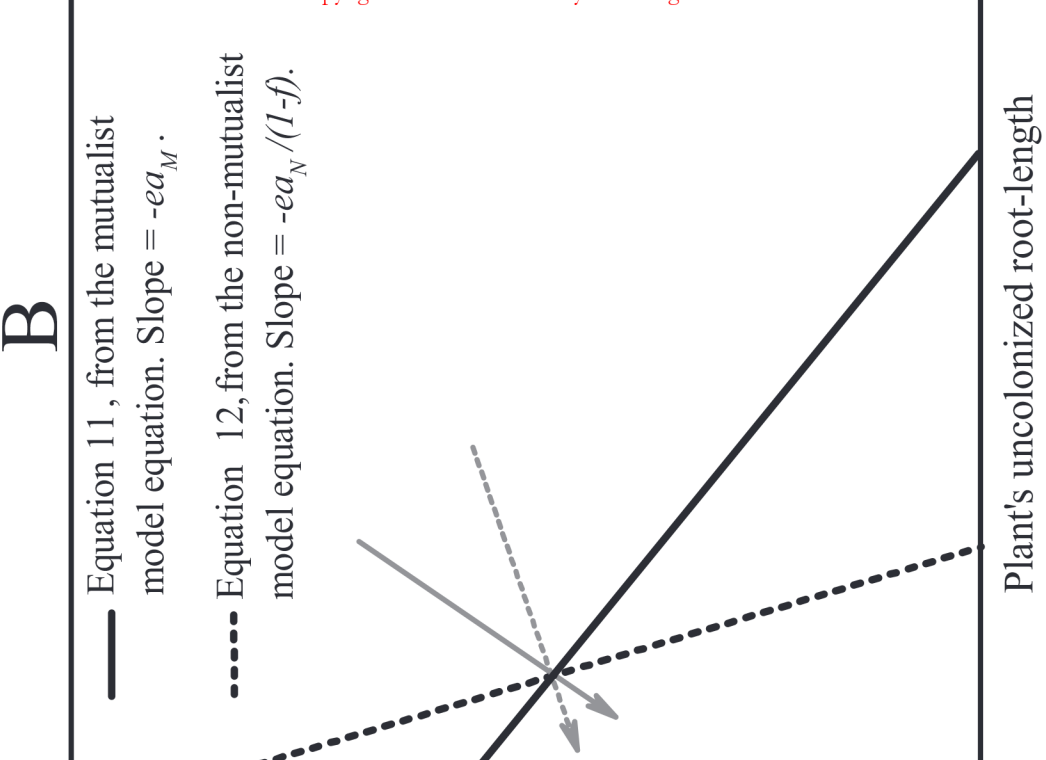
higher root growth rate, D, brings about a wider range of f for which coexistence can occur. Changing cost

of mutualism (s) has negligible effect on the difference between fidelity $(f_{\min} \sim f_{\max})$ as shown in (A, B)

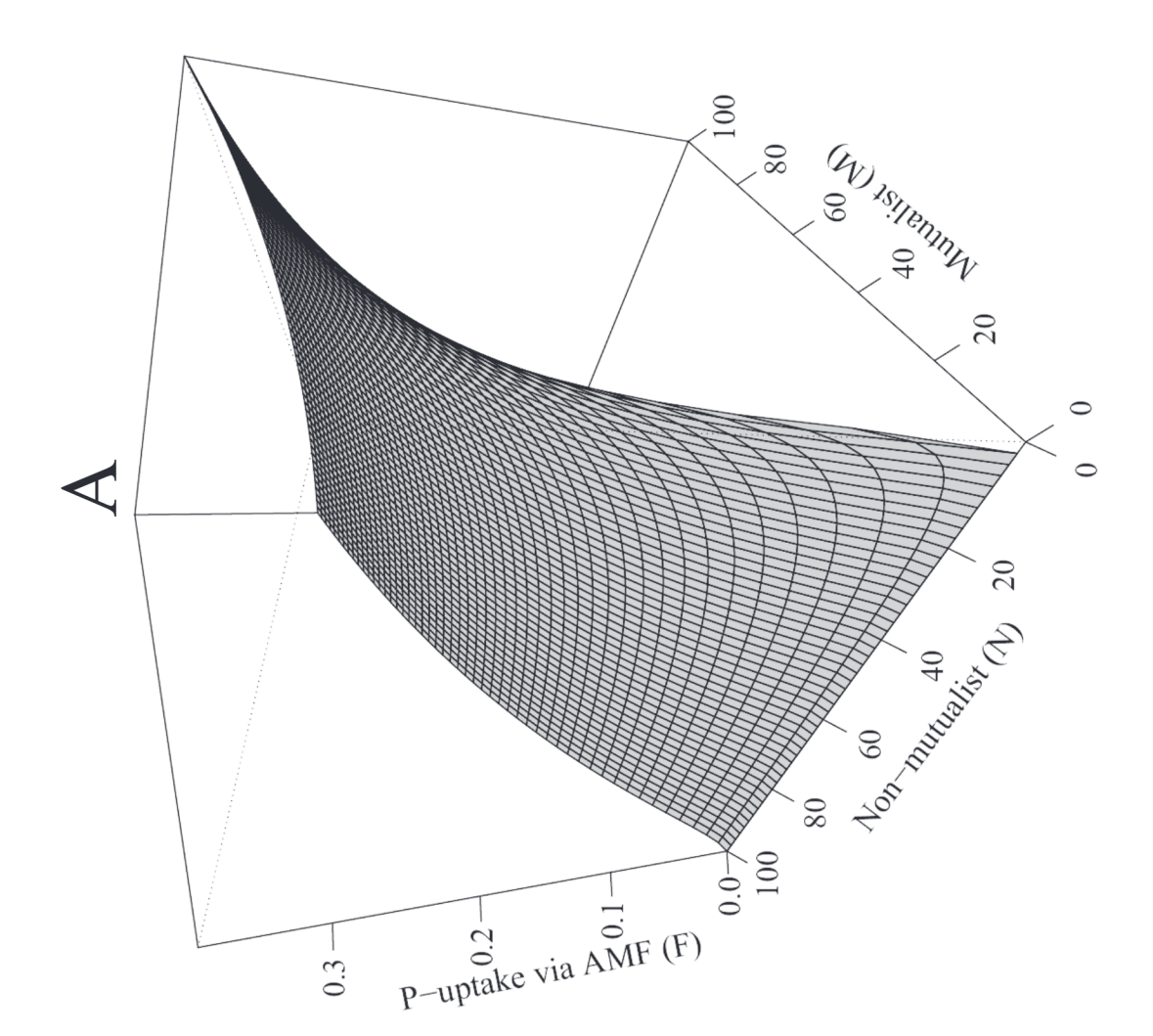
or (C, D) but increasing the ratio of the colonization rates (a_M/a_N) decreases the maximum fidelity limit

 (f_{max}) considerably in (A, C) or (B, D).





Preferenial allocation rate scaled by symbiont density



is is the author's accepted manuscript without opyediting, formatting, or final corrections. It will be published in its final form in an upcoming issue of The American Naturalist, published by The University of Chicago Press. Include the DOI when citing or anothing: https://doi.org/10.1086/718643 This is the author's accepted manuscript without opyediting, formatting Copyright 2021 The Univer**so**y of Chicago Press. 09 3.0 rate of preferential scaled by symbiont density (Â/ Eq. 11, from the C-allocation, A 50 2.5 mutualist model equation. length of Preferential allocation rate new roots, R 40 Eq. 12, from the 100 2.0 mutualist, M non-mutualist model equation. 30 non-mutualist, N 1.5 20 50 1.0 10 0.5 100 200 300 400 500 600 200 400 800 1000 600 Plant's uncolonized root-length (R) time $f_{\min} < f < f_{\max}$ scaled by symbiont density $({\hat A}/{\hat lpha})$ 150 3.0 09 rate of preferential Eq. 11, from the C-allocation, A 2.5 mutualist model equation. Preferential allocation rate length of new roots, R Eq. 12, from the 40 100 2.0 non-mutualist model equation. mutualist, M 30 1.5 non-mutualist, N 20 50 1.0 10 0.5 0.0 0 100 200 300 400 500 400 200 600 800 1000 Plant's uncolonized root-length (R) time $f > f_{\text{max}}$ E F scaled by symbiont density $({\rm \^A}/{\rm \^A})$ 150 3.0 rate of preferential 09 Eq. 11, from the C-allocation, A 2.5 mutualist model equation. Preferential allocation rate length of 50 new roots, R Eq. 12, from the 100 2.0 40 mutualist, M non-mutualist model equation. 30 non–mutualist, N 1.5 20 50 1.0 10 0.5

300

Plant's uncolonized root-length (R)

200

100

400

500

200

400

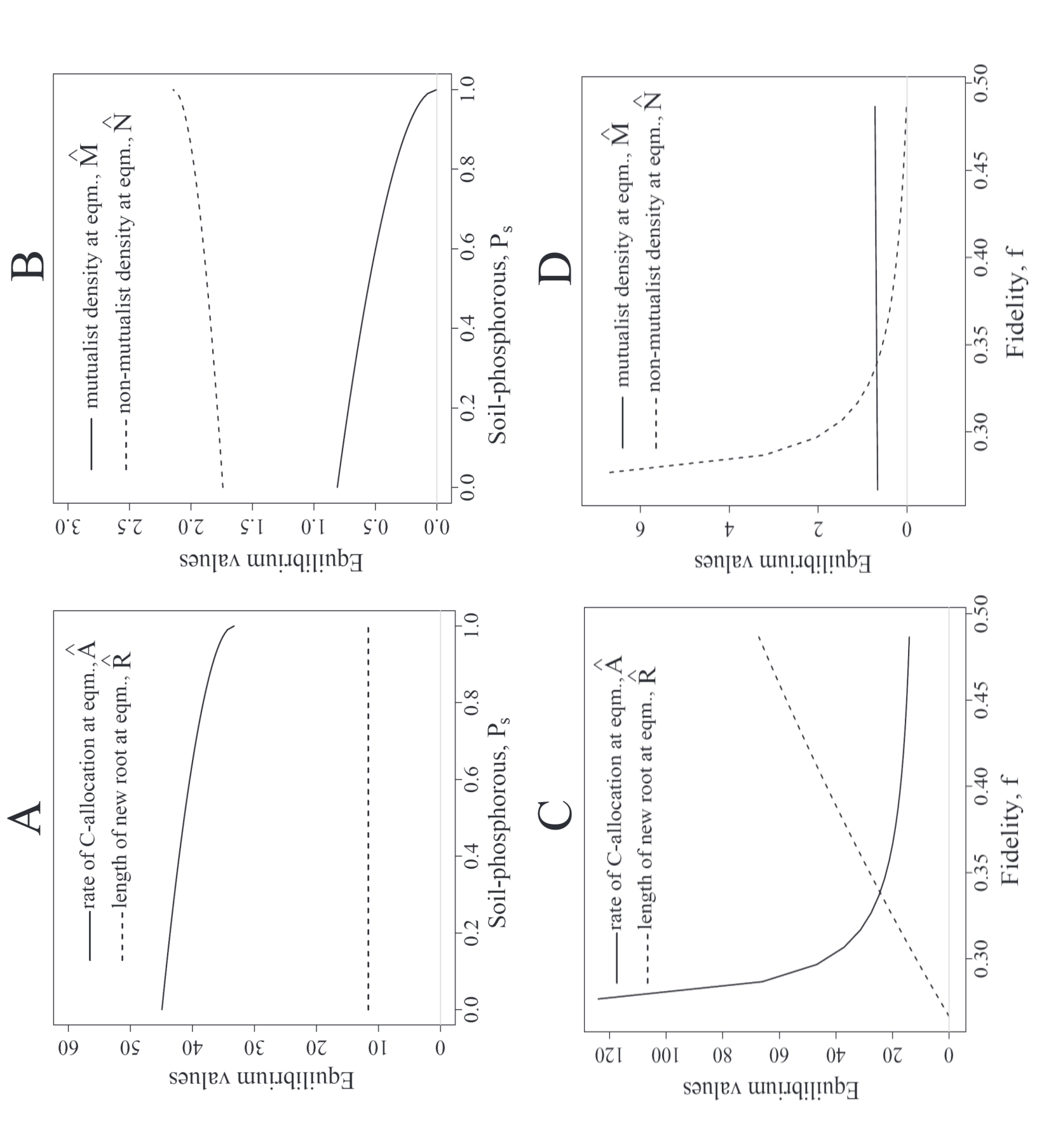
time

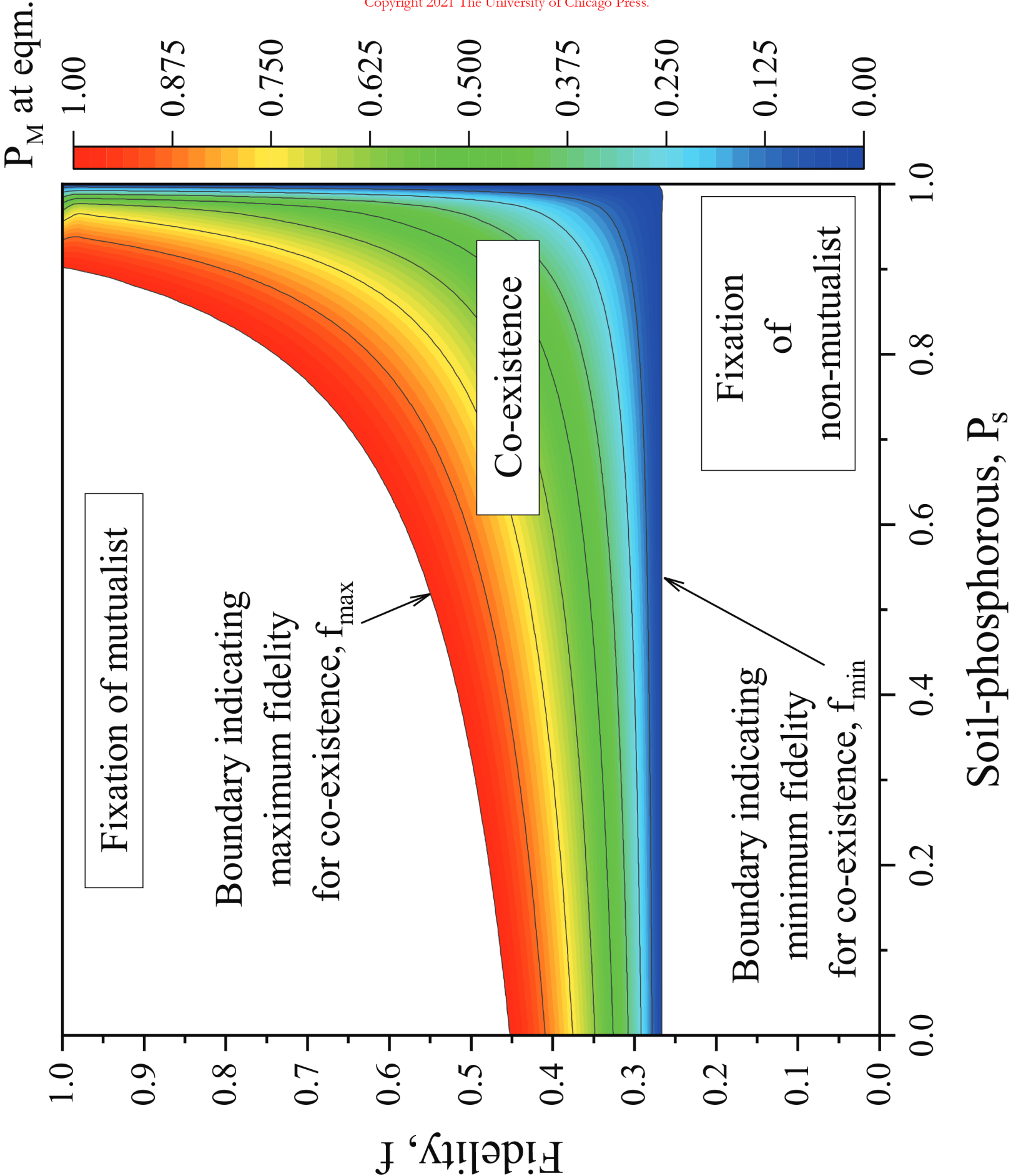
600

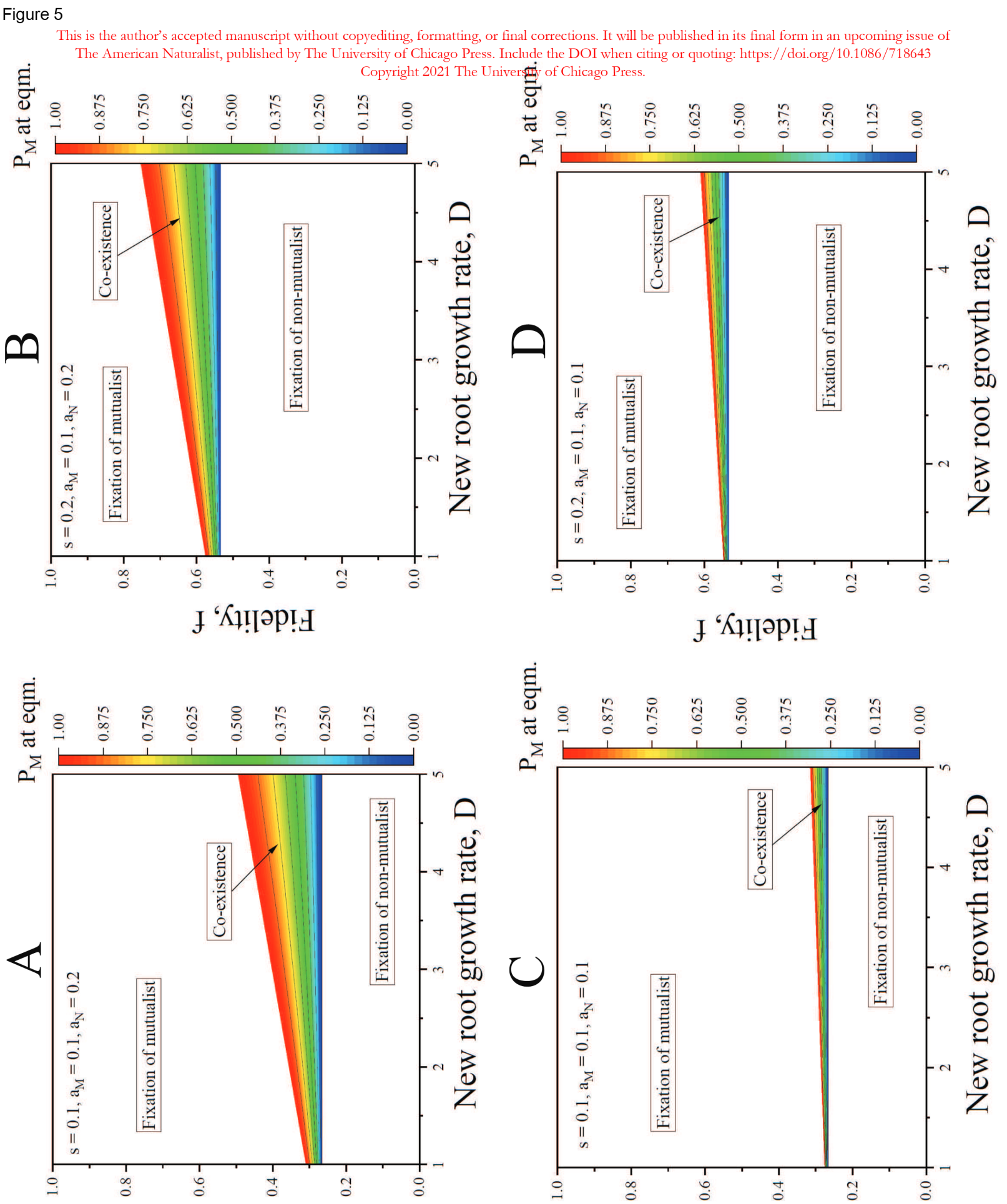
800

0.0

1000







1.0-

Fidelity, f

0.4

Fidelity, f

0.2

9.0

This is the author's accepted manuscript without copyediting, formatting or final corrections. It will be published in its final form in an upcoming issue of Short title. Symbiont competition and coexistence The American Naturalist, published by The University of Chicago Press. Include the DOI when citing or quoting: https://doi.org/10.1086/718643

Copyright 2021 The University of Chicago Press.

Supplementary material for "Preferential allocation of benefits and resource competition among recipients allows coexistence of symbionts within hosts"

Shyamolina Ghosh¹, Dan

Daniel C. Reuman^{1,2},

James D. Bever^{1,*}

¹Department of Ecology and Evolutionary Biology and Kansas Biological Survey, The University of Kansas, 1200 Sunnyside Avenue, Lawrence, KS, 66045, USA

²Laboratory of Populations, Rockefeller University, 1230 York Ave, New York, NY, 10065, USA

*corresponding author: jbever@ku.edu

Journal: The American Naturalist

S1 Assumptions on model parameter values

We adopt the following biologically reasonable assumptions:

- 1. 0 < f < 1;
- 2. $a_N \ge a_M > 0$;
- 3. s > 0;
- 4. $b_{\text{max}} d > 0$;
- 5. $b_{\text{max}}(1-s) d > 0$;
- 6. $0 < P_S < 1$;
- 7. D > 0;
- 8. 0 < e < 1;
- 9. 0 < u < 1;
- 10. $K_A > 0$;
- 11. K > 0.

These assumptions are referred to by number in the derivations that follow.

S2 Model equilibrium

A positive equilibrium of the dynamical model, here denoted $\hat{A} > 0, \hat{R} > 0, \hat{M} > 0, \hat{N} > 0$, occurs if and only if a positive solution exists to the the system of equations obtained by setting the right sides of (1),(2),(3),(4) in the main text to 0. So we examine that system of equations. Setting $\frac{dM}{dt} = 0$ and $\frac{dN}{dt} = 0$, substituting in the expressions for C_M and C_N , and carrying out algebraic manipulations leads to

$$\frac{\hat{A}}{\hat{\alpha}} = -ea_M \hat{R} + \frac{Kd}{b_{\text{max}}(1-s) - d} \tag{S1}$$

$$\frac{\hat{A}}{\hat{\alpha}} = \frac{-ea_N}{1-f}\hat{R} + \frac{Kd}{(b_{\text{max}} - d)(1-f)},$$
(S2)

where

$$\hat{\alpha} = (\hat{M} + \hat{N}) \left[1 - f + f \frac{\hat{M}}{\hat{M} + \hat{N}} \right]. \tag{S3}$$

Therefore we consider the two lines in xy-space given by

$$y = -ea_M x + \frac{Kd}{b_{\text{max}}(1-s) - d}$$
(S4)

$$y = \frac{-ea_N}{1 - f}x + \frac{Kd}{(b_{\text{max}} - d)(1 - f)}.$$
 (S5)

The x-intercepts of these lines are $\frac{Kd}{ea_M(b_{\max}(1-s)-d)}$ and $\frac{Kd}{ea_N(b_{\max}-d)}$, respectively. By assumption 2 listed above, $\frac{a_N}{a_M} \geq 1$, and by assumptions 3-5, $\frac{b_{\max}(1-s)-d}{b_{\max}-d} < 1$. So therefore $\frac{a_N}{a_M} > \frac{b_{\max}(1-s)-d}{b_{\max}-d}$, and therefore $\frac{Kd}{ea_M(b_{\max}(1-s)-d)} > \frac{Kd}{ea_N(b_{\max}-d)}$, i.e. the x-intercept of (S4) is strictly to the right of the x-intercept of (S5). Likewise, by assumption 1 and 2, the line given by (S5) is steeper (has a more-negative slope) than the line give by (S4). So the two lines have a positive intersection point if and only if the y-intercept of (S5) is strictly greater than the y-intercept of (S4), i.e.,

$$\frac{Kd}{b_{\max}(1-s) - d} < \frac{Kd}{(b_{\max} - d)(1-f)}.$$
 (S6)

After some algebra, this becomes

$$f > \frac{b_{\text{max}}s}{b_{\text{max}} - d}.$$
 (S7)

The condition (S7) is our first necessary condition for the existence of a positive equilibrium to the model dynamical equations ((1)-(4) in the main text). We denote $f_{\min} = \frac{b_{\max}s}{b_{\max}-d}$. By assumption 5, $b_{\max}(1-s) - d > 0$, so $d < b_{\max}(1-s)$, so $d < b_{\max} - b_{\max}s$, so $b_{\max}s < b_{\max} - d$, so $f_{\min} < 1$. Thus no additional assumptions are needed to conclude that (S7) can be satisfied for some 0 < f < 1.

If the condition (S7) is satisfied, then there is a positive solution to (S4)-(S5), giving us (after some algebra) the positive quantities

$$\hat{R} = \frac{Kd(1-f)}{e(a_N - a_M(1-f))} \left[\frac{1}{(b_{\text{max}} - d)(1-f)} - \frac{1}{b_{\text{max}}(1-s) - d} \right]$$
(S8)

$$= \frac{Kd(f - f_{\min})}{e(a_N - a_M(1 - f))(b_{\max} - d)(1 - f_{\min})}$$
 (S9)

$$\frac{\hat{A}}{\hat{\alpha}} = \frac{Kd(b_{\text{max}} - d)(a_N - a_M) + sKdb_{\text{max}}a_M}{(b_{\text{max}} - d)(b_{\text{max}}(1 - s) - d)(a_N - a_M(1 - f))}.$$
(S10)

We can also see directly that these are positive, using the assumptions listed above.

Now, setting $\frac{dA}{dt} = 0$, we get

$$0 = 1 - P_S - \hat{A}F(\hat{M}, \hat{N}) \tag{S11}$$

$$\hat{A} = \frac{1 - P_S}{F(\hat{N}, \hat{M})} \tag{S12}$$

$$= \frac{(1 - P_S)\hat{\alpha}}{u\left(\frac{\hat{M}}{K_A + \hat{M}}\right)\hat{M}} \tag{S13}$$

$$=\frac{(1-P_S)\hat{\alpha}(K_A+\hat{M})}{u\hat{M}^2},\tag{S14}$$

which leads to the quadratic equation

$$u\frac{\hat{A}}{\hat{\alpha}}\hat{M}^2 - (1 - P_S)\hat{M} - (1 - P_S)K_A = 0.$$
 (S15)

The solutions to this quadratic equation are

$$\hat{M} = \frac{(1 - P_S) \pm \sqrt{(1 - P_S)^2 + 4u\frac{\hat{A}}{\hat{\alpha}}(1 - P_S)K_A}}{2u\frac{\hat{A}}{\hat{\alpha}}}.$$
 (S16)

But, by assumptions 6, 9 and 10,

$$4u\frac{\hat{A}}{\hat{\alpha}}(1-P_S)K_A > 0, \tag{S17}$$

SO

$$(1 - P_S)^2 + 4u\frac{\hat{A}}{\hat{\alpha}}(1 - P_S)K_A > (1 - P_S)^2,$$
(S18)

so

$$\sqrt{(1 - P_S)^2 + 4u\frac{\hat{A}}{\hat{\alpha}}(1 - P_S)K_A} > 1 - P_S, \tag{S19}$$

so the solution

$$\hat{M} = \frac{(1 - P_S) - \sqrt{(1 - P_S)^2 + 4u_{\hat{\alpha}}^{\hat{A}}(1 - P_S)K_A}}{2u_{\hat{\alpha}}^{\hat{A}}}$$
 (S20)

is negative. Since we are looking for positive solutions, we ignore this one, considering only

$$\hat{M} = \frac{(1 - P_S) + \sqrt{(1 - P_S)^2 + 4u\frac{\hat{A}}{\hat{\alpha}}(1 - P_S)K_A}}{2u\frac{\hat{A}}{\hat{\alpha}}},$$
 (S21)

which is positive, by the assumptions.

Now setting $\frac{dR}{dt} = 0$, we get

$$0 = D - (a_N \hat{M} + a_N \hat{N})\hat{R}. \tag{S22}$$

Solving for \hat{N} gives

$$\hat{N} = \frac{D}{a_N \hat{R}} - \frac{a_M}{a_N} \hat{M}. \tag{S23}$$

This is positive whenever

$$\hat{M}\hat{R} < \frac{D}{a_M}.\tag{S24}$$

In the limit as $f \to f_{\min}$ from the right, $\hat{R} \to 0$ from above, so (S24) is satisfied for f sufficiently close to f_{\min} . The derivative of \hat{R} with respect to f, computed starting from (S9), is

$$\frac{d\hat{R}}{df} = \frac{Kd}{e(b_{\text{max}} - d)(1 - f_{\text{min}})} \frac{f_{\text{min}} a_M + a_N - a_M}{(f a_M + a_N - a_M)^2},\tag{S25}$$

which is positive, by the assumptions. Therefore \hat{R} increases as f increases from f_{\min} . Likewise, setting

$$\eta = \frac{\hat{\alpha}}{\hat{A}} \tag{S26}$$

$$= \frac{a_M(b_{\text{max}} - d)(b_{\text{max}}(1 - s) - d)f + (a_N - a_M)(b_{\text{max}} - d)(b_{\text{max}}(1 - s) - d)}{Kd(b_{\text{max}} - d)(a_N - a_M) + sKdb_{\text{max}}a_M},$$
 (S27)

we can write

$$\hat{M} = \frac{1 - P_S}{2u} \eta + \frac{1}{2u} \sqrt{(1 - P_s)^2 \eta^2 + 4u(1 - P_S) K_A \eta}.$$
 (S28)

Again making use of the assumptions listed above, it is straightforward to see that η is a linear, positive-slope function of f, and therefore increases as f increases. But (S28) indicates that \hat{M} increases as η increases, so \hat{M} increases as f increases from f_{\min} . Thus the condition (S24) is satisfied for f up to some value, and then is not satisfied for f equal to that value or higher than that value. We take f_{\max} to be the minimum of this value and 1. Although we have not computed a closed-form solution for f_{\max} , for any specific values of model parameters it would be straightforward and computationally fast to compute f_{\max} to any desired precision by computing \hat{M} and \hat{R} for a range of values of f increasing from f_{\min} , and then evaluating for which values the condition (S24) is satisfied.

In summary, the calculations here indicate that $f_{\min} < f < f_{\max}$ is a necessary and sufficient condition for the existence of a positive equilibrium of the model dynamical equations ((1)-(4) in the main text). The equilibrium is then given by

$$\hat{R} = \frac{Kd(f - f_{\min})}{e(a_N - a_M(1 - f))(b_{\max} - d)(1 - f_{\min})}$$
(S29)

$$\frac{\hat{A}}{\hat{\alpha}} = \frac{Kd(b_{\text{max}} - d)(a_N - a_M) + sKdb_{\text{max}}a_M}{(b_{\text{max}} - d)(b_{\text{max}}(1 - s) - d)(a_N - a_M(1 - f))}$$
(S30)

$$\hat{M} = \frac{(1 - P_S) + \sqrt{(1 - P_S)^2 + 4u_{\hat{\alpha}}^{\hat{A}}(1 - P_S)K_A}}{2u_{\hat{\alpha}}^{\hat{A}}}$$
(S31)

$$\hat{N} = \frac{D}{a_N \hat{R}} - \frac{a_M}{a_N} \hat{M} \tag{S32}$$

$$\hat{A} = \frac{\hat{A}}{\hat{\alpha}}(\hat{M} + (1 - f)\hat{N}). \tag{S33}$$

For any given values of the parameters (1)-(4) in the main text, the model equilibrium can be obtained straightforwardly by evaluating these expressions in turn.

S3 Stability of the model equilibrium

We evaluated the local asymptotic stability of the model equilibrium numerically, as follows. We selected model parameters within the ranges specified by Table S1, independently and following uniform distributions across the specified ranges for each parameter. For each set of parameters that satisfied the assumptions listed above (section S1) we computed the range of f values f_{\min} to f_{\max} . The bound f_{\max} was estimated with a root-finding algorithm in the R programming language (the function 'uniroot' in the

Table S1: Ranges used for model parameters in evaluating stability of the equilibrium. See section S3.

Parameter	Lower	Upper	
u	0.001	1	
$b_{ m max}$	0.001	5	
d	0.001	5	
s	0.001	0.999	
e	0.001	0.999	
a_M	0.001	5	
a_N	0.001	5	
D	0.001	5	
K_A	0.01	15	
K	0.01	15	
P_S	0.001	0.999	

'stats' package) which had very good but finite precision. If the imprecision for $f_{\rm max}$ reported by uniroot was more than 1/50th the distance between $f_{\rm min}$ and $f_{\rm max}$, parameters were not used. Otherwise, 27 values of f were spaced evenly from $f_{\rm min}$ and $f_{\rm max}$, the first and last were discarded (these were $f_{\rm min}$ and $f_{\rm max}$ themselves), and the other f values were combined with values for the other parameters. For these parameter sets, the model Jacobian was calculated at the equilibrium, eigenvalues of the Jacobian were computed using the 'eigen' function in R, and the maximal real part of these eigenvalues was retained. If this real part was negative, the model equilibrium for those parameters was stable. Stability was checked for 297925 parameter combinations, and in every case the model equilibrium was stable. Although this does not guarantee that the model equilibrium we described (section S2) is always stable, it does indicate that stability is common for reasonable model parameters.

S4 Alternative form of the efficiency of phosphorus return in Eq. 1 of main text

Here we start by rewriting the functional form of phosphorus return from Eq. (1) of main text as follows:

$$F(M,N) = u\left(\frac{M}{M+K_A}\right) \left\{ \frac{M/(M+N)}{1-f+f\{M/(M+N)\}} \right\}$$
 (S34)

or,
$$F(M,N) = F_1(M,N) = u\left(\frac{M}{M+K_A}\right) \left\{\frac{M}{M+N(1-f)}\right\}$$
 (S35)

One can consider a simpler and alternative form for F(M, N) in Eq. (1) as follows;

$$F(M,N) = u\left(\frac{M}{M+K_A}\right)\left\{f + (1-f)\left(\frac{M}{M+N}\right)\right\}$$
 (S36)

or,
$$F(M,N) = F_2(M,N) = u\left(\frac{M}{M+K_A}\right)\left\{\frac{M+Nf}{M+N}\right\}$$
 (S37)

F(M,N) from Eq. S37 is depicted in Fig. S1 and its shape is very similar to Fig. 1(a) in the main text. We simulated Eqs. (1) - (7) of main text with $F_2(M,N)$ as F(M,N) in Eq. (5) and got qualitatively same results as of Fig. 2 in the main text. This happened because the two terms F_1 and F_2 are same at equilibrium (see Table S2) for $f \to 0$, $f \to f_{min}$, $f \to f_{max}$ and $f \to 1$. Therefore, we can say that our finding is robust in nature.

Table S2: Comparing two functional forms at the equilibrium. See section S4.

F(M,N) at eqm.	when $f \to 0$	when $f \to f_{min}$	when $f \to f_{max}$	when $f \to 1$
$F_1(\hat{M},\hat{N}) \rightarrow$	$u\left(\frac{\hat{M}}{\hat{M}+K_A}\right)\left(\frac{\hat{M}}{\hat{M}+\hat{N}}\right)$	0	$u\left(\frac{\hat{M}}{\hat{M}+K_A}\right)$	$u\left(\frac{\hat{M}}{\hat{M}+K_A}\right)$
$F_2(\hat{M},\hat{N}) \to$	$u\left(\frac{\hat{M}}{\hat{M}+K_A}\right)\left(\frac{\hat{M}}{\hat{M}+\hat{N}}\right)$	0	$u\left(\frac{\hat{M}}{\hat{M}+K_A}\right)$	$u\left(\frac{\hat{M}}{\hat{M}+K_A}\right)$

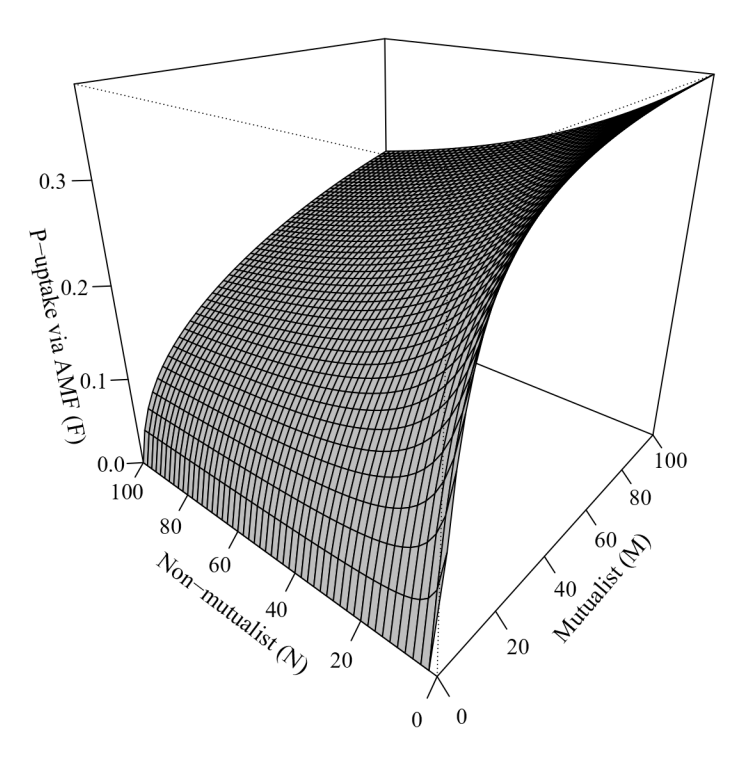


Figure S1: P-uptake via mycorrhizal fungi, $F_2(M, N)$ as a saturating function of densities of mutualists (M) and non-mutualists (N) (Eq. S37). Parameters used: $f = 0.3, u = 0.4, K_A = 5$.